# Zero-TPrune: Zero-Shot Token Pruning through Leveraging of the Attention Graph in Pre-Trained Transformers

Hongjie Wang, Bhishma Dedhia, Niraj K. Jha

Department of Electrical & Computer Engineering Princeton University Princeton, NJ 08544 {hongjie,bdedhia,jha}@princeton.edu

# **Abstract**

Since their invention, Transformers have shown strong transfer learning capability and significant learning capacity in various application domains. However, deployment of Transformer models on the edge is increasingly challenging due to the exponentially growing model size and inference cost that scales quadratically with the number of tokens in the input sequence. Token pruning is an emerging solution to address this challenge due to its ease of deployment on various Transformer backbones. However, most token pruning methods require a computationallyexpensive fine-tuning process after or during pruning, which is not desirable in many cases. Some recent works explore pruning of off-the-shelf pre-trained Transformers without fine-tuning. However, they only take the importance of tokens into consideration. In this work, we propose Zero-TPrune, the first zero-shot method that considers both the importance and similarity of tokens in performing token pruning. Zero-TPrune leverages the attention graph of pre-trained Transformer models to produce an importance rank for tokens and removes the less informative tokens. The attention matrix can be thought of as an adjacency matrix of a directed graph, to which a graph shift operator can be applied iteratively to obtain the importance score distribution. This distribution guides the partition of tokens into two groups and measures similarity between them. Due to the elimination of the fine-tuning overhead, Zero-TPrune can easily prune large models and perform hyperparameter tuning efficiently. We evaluate the performance of Zero-TPrune on vision tasks by applying it to various vision Transformer backbones. Zero-TPrune reduces the computational cost of off-the-shelf pre-trained Transformers by more than 20% with less than 0.4% accuracy loss. Compared with state-of-the-art pruning methods that require fine-tuning, Zero-TPrune not only eliminates the need for fine-tuning after pruning, but does so with only around 0.3% accuracy loss. Compared with state-of-the-art fine-tuning-free pruning methods, Zero-TPrune reduces accuracy loss by up to 45% on medium-sized models.

## 1 Introduction

In the past decade, machine learning algorithms have demonstrated excellent performance in various fields, including computer vision (CV) [1], natural language processing (NLP) [2], robotics [3], games [4], etc. In 2017, a brand new machine learning model, called Transformer [5], emerged and exhibited outstanding performance on various NLP tasks. Compared with previous convolutional neural network (CNN) and recurrent neural network (RNN) based language models, Transformers simultaneously achieved higher accuracy and better computational parallelism. Transformers were also shown to outperform state-of-the-art CNNs on CV tasks [6] due to their large learning capacity and strong transfer learning capability. The latter enables extremely large Transformer-based models

to be pre-trained on upstream tasks and then fine-tuned for excellent performance on downstream tasks. However, these models have kept growing larger, with recent models containing hundreds of billions or even trillions of parameters [7]. Thus, it is increasingly challenging to efficiently deploy these models on the edge and target real-time inference under energy, memory, and computational resource constraints.

Pruning is a popular technique to address the above challenge. At the heart of a Transformer layer, a multi-head self-attention mechanism enables each token in the input sequence to attend to every other token, whose computation complexity is quadratic in the input sequence size. This poses a large hurdle when Transformers need to process long input sequences. However, it also provides possibilities for pruning. For instance, head pruning [8] removes redundant heads in each Transformer layer to decrease model size. An orthogonal approach that we consider in this article is token pruning, which removes unimportant tokens in the input sequence to reduce computational cost. The intuition behind this method is that for CV tasks such as image recognition, not all parts in the input images are important or necessary to obtain a successful inference. Note that token pruning does not change the architecture of the Transformer. It only prunes the information that passes through the sequential layers of the Transformer. This characteristic of token pruning enables it to be applied to various Transformer backbones, and the resultant sparsity can be fully exploited by any computational hardware. However, most previous token pruning methods require computationally-expensive training or fine-tuning after pruning, which is often undesirable. For example, DynamicViT [14] requires 150 hours of fine-tuning on NVIDIA A100 GPU to prune the DeiT-S [16] model. Moreover, the memory and computational resources available may differ widely between edge devices; they may also have wide variations in throughput requirements. The methods mentioned above need the model to be trained repeatedly after setting different pruning configurations to adapt to the underlying hardware constraints, making the pruning process even more expensive. In addition, these methods are impractical for pruning very large models due to the high computation overhead of training after pruning. For instance, hundreds or even thousands of GPU hours on NVIDIA A100 are needed to apply DynamicViT [14] to the DeiT-B and DeiT-L models [16].

In this work, we propose a zero-shot token pruning method called Zero-TPrune. It uses the attention graph of pre-trained Transformers to rank the importance of tokens and guide token partitioning for similarity measurements. Zero-TPrune is composed of an **I-stage** and **S-stage**, focusing on the importance and similarity of tokens, respectively. Although Zero-TPrune can potentially be applied to any Transformer-based tasks, we focus on vision tasks to evaluate its performance in this article. We illustrate the superiority of our method on ImageNet [17] using various backbones, including DeiT [16], LV-ViT [18], AugReg [26], etc. Experimental results show that Zero-TPrune achieves accuracy comparable to state-of-the-art Transformer pruning methods while eliminating the need for training after pruning. This is enabled through highly efficient utilization of the feature identification ability of pre-trained Transformer models. Note that Zero-TPrune does not require fine-tuning of the model after pruning; in other words, it achieves zero-shot token pruning. It can be applied to large models easily due to its low cost.

The main contributions of this work can be summarized as follows. (1) We present Zero-TPrune, a zero-shot token pruning method that efficiently leverages the feature identification capability (manifested through the attention graph and embedded token vectors) of pre-trained Transformers. It exploits both the importance and similarity of tokens to perform pruning. (2) We consider the attention matrix as an adjacency matrix of a directed graph and use a graph signal to represent the importance score distribution on tokens. We propose a Weighted Page Rank (WPR) algorithm to reduce noise from unimportant tokens during importance assignment. (3) To account for similarity between tokens, we partition tokens into two groups and perform similarity-based matching and pruning. Guidance from importance distribution improves the precision of this process. (4) We apply Zero-TPrune and baseline methods to various Transformer backbones and evaluate their performance on ImageNet. We show that compared with state-of-the-art fine-tuning-required Transformer pruning methods, Zero-TPrune eliminates the need for fine-tuning after pruning DeiT-S with only around 0.3% accuracy reduction. Zero-TPrune reduces accuracy loss by 31% on DeiT-S when compared with state-of-the-art fine-tuning-free methods.

This article is organized as follows. We discuss previous works related to vision Transformers and Transformer pruning in Section 2. We describe our pruning methodology in Section 3. We present ablation experiments of our method and compare it with state-of-the-art methods in Section 4. We provide a summary and suggest future work in Section 5.

## 2 Related Works

In the first few years after the Transformer model was proposed in 2017, it was mainly employed in the NLP field [2]. ViT [6] was the first work to directly apply an *encoder-only* Transformer architecture to non-overlapping image patches in an image classification task without employing any convolution operations. Relative to state-of-the-art CNNs, ViT was able to achieve better performance through large-scale pre-training. DeiT [16] was another convolution-free Transformer that was trained only on ImageNet [17] and achieved better performance than ViT by relying on several training techniques. Both ViT and its follow-up architectures split the input image into multiple non-overlapping image patches and transform them into tokens for further processing. This provides a new dimension to sparsity exploitation that is quite different from sparsity-enhancing techniques employed in CNNs.

Most of the previous token pruning works focus on NLP tasks, including PoWER-BERT [9], Length-Adaptive Transformer [10], SpAtten [11], TR-BERT [12], and Learned Token Pruning [13]. For CV tasks, a typical token pruning work is DynamicViT [14]. It inserts prediction modules between transformer blocks to predict and drop less informative tokens. The prediction modules are neural networks that can be jointly trained with the vision Transformer backbone. Instead of using a deterministic strategy to prune tokens, A-ViT [15] introduces a stochastic pruning process. It uses adaptive halting modules to compute the halting probability per token. A token is pruned (i.e., discarded) upon reaching the halting condition. As a result, the number of tokens is gradually reduced, leading to faster inference. Although the pruning methods mentioned above require few or even no extra parameters for pruning, they require computationally-expensive fine-tuning after pruning. On the contrary, our proposed Zero-TPrune is able to eliminate the training process after pruning with only 0.3% accuracy reduction.

There are a few previous works that have explored pruning tokens without requiring fine-tuning. ATS [21] uses an inverse transform to accomplish adaptive token sampling based on the importance score distribution. When the importance scores are concentrated on several tokens, the number of sampled tokens automatically reduces. However, ATS only uses the attention probability of the classification (CLS) token in the attention matrix and ignores the effect of similarity between tokens. ToMe [23], on the other hand, focuses on merging tokens instead of pruning them, thereby reducing the inference overhead of pre-trained Transformers without fine-tuning. Tokens are progressively merged based on their similarity as the layers become deeper. However, ToMe solely relies on embedding vectors from pre-trained models and its matching process lacks proper guidance (more details in Section 3.3). In contrast, our proposed method, Zero-TPrune, effectively utilizes both the complete attention matrix and embedding vectors from pre-trained Transformers, while simultaneously considering the importance and similarity of tokens.

# 3 Methodology

In this section, we first provide an overview of our proposed methodology, Zero-TPrune, in Section 3.1, then describe its components (**I-stage** and **S-stage**) in detail. We give a review of the attention probability matrix employed in vision Transformers in Supplementary Material Section B. Based on treating this matrix as an adjacency matrix of a directed graph, we propose the WPR algorithm to calculate the importance score of each token via iterative graph signal transformation in the **I-stage**. This is discussed in Section 3.2. To measure similarity between tokens and perform pruning based on this similarity, we introduce the **S-stage** and discuss potential design choices in Section 3.3. Note that Zero-TPrune is potentially differentiable, which enables the pruned model to be further fine-tuned for better performance. This optional training-after-pruning paradigm is described in Supplementary Material Section C.

## 3.1 Overview: Zero-TPrune

The overall Zero-TPrune framework is shown in Fig. 1. Each pruning layer is composed of multiple stages and can be inserted anywhere between Transformer blocks. The **I-stage** and **S-stage** enable Zero-TPrune to take both importance and similarity into consideration. The objective of the **I-stage** is to obtain an importance score distribution on tokens and retain the top-k important tokens. To achieve this objective, we propose the WPR algorithm and use the attention matrix from the pre-trained Transformer block. In the **S-stage**, we measure similarity between tokens based on their embedding vectors and retain only one token in each similar pair. To have better control over the characteristics of paired tokens and reduce computational overheads, we partition tokens into two groups, guided by their importance rank. Tokens in the same group are never paired to measure similarity.

A straightforward way to combine the two stages is to consecutively connect the **I-stage** and **S-stage**: some tokens are pruned based on the obtained importance score distribution in the **I-stage**; this

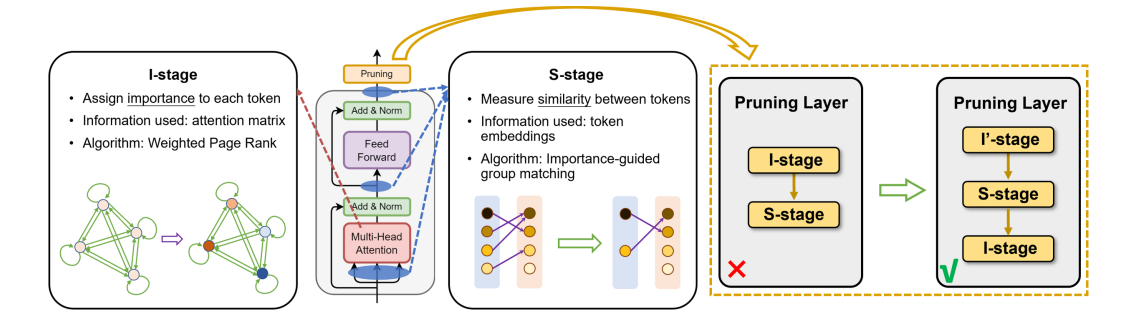


Figure 1: The overall framework of Zero-TPrune. Pruning layers can be inserted between any Transformer blocks to reduce the number of tokens. Each pruning layer is composed of an I'-stage, I-stage, and S-stage.

distribution is then used to guide the partition in the **S-stage** and some other tokens are pruned based on similarity. However, such a trivial combination may *overwhelm the major group* in the **I-stage**. In this stage, each token votes for "more important tokens" and the weight of their votes is determined by their importance in the last round of voting. Besides the "really important" tokens, tokens also intend to vote for tokens *that are similar to them*. When ground truth important tokens are only a small part of an image and unimportant background tokens dominate, sometimes background tokens vote for each other and gradually obtain high importance scores after multiple rounds of voting. Details of this phenomenon can be found in Supplementary Material Section A.1.

We resolve this issue by interchanging the **I-stage** and **S-stage**. This method enables the early elimination of similar tokens in the **S-stage**, consequently reducing the adverse impact of similarity in the **I-stage** to a significant extent. We present a comparison of the two patterns in Supplementary Material Section A.2. To facilitate partitioning in the **S-stage**, we introduce a pre-ranking **I'-stage** to assign importance scores to tokens with a *single* round of voting. Notably, no token is pruned in the **I'-stage**. Consequently, the pruning layer comprises consecutively connected **I'-stage**, **S-stage**, and **I-stage**.

## 3.2 I-stage: Importance-based Pruning

To retain the top-k important tokens, we first need to define a metric that distinguishes unimportant tokens from important ones. This metric is called the *importance score*. In order to obtain the importance score, we treat attention matrix  $\mathbf{A}^{(h,l)}$  as the adjacency matrix of a directed graph, called the *attention graph*, as shown in Fig. 2(a). We wish to use the information in this graph to assign an importance score to each token (node) and remove the unimportant ones. This is challenging because of several reasons. (i) The attention graph is complex. The graph is directed and fully-connected, and usually includes hundreds of nodes when the input is an image. (ii) We have a strict constraint on the computational overhead incurred by the algorithm. For different inputs, a different set of tokens needs to be pruned during inference.

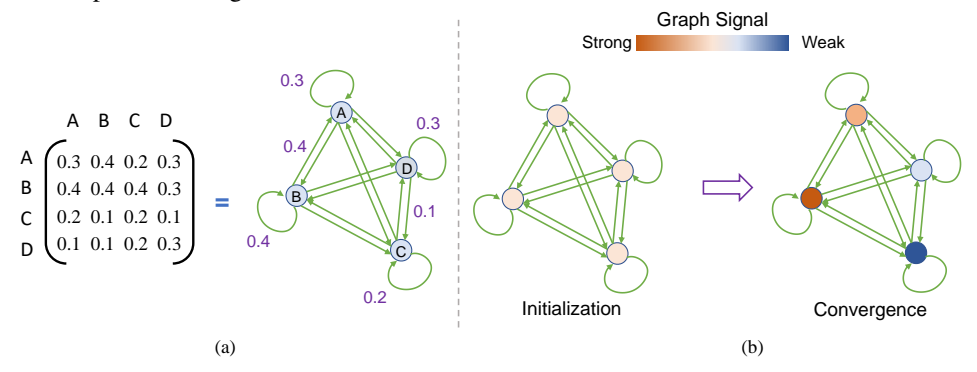


Figure 2: Overview of the I-stage: (a) from a  $4\times4$  attention matrix to an attention graph and (b) graph signal transformation from initialization to convergence period.

Inspired by the Page Rank [20] algorithm, we propose a WPR algorithm to derive the importance scores. Page Rank is, of course, famously used in Google Search for ranking web pages. In the original Page Rank algorithm, links between web pages are unweighted. In order to apply it to

the weighted and directed attention graph, we consider the signal of each node in this graph as the importance of each token. We initialize the graph signal uniformly. Then, we use the adjacency matrix as a graph shift operator (GSO). When the GSO is applied to the graph signal, each node votes for which node is more important through the weight assigned to output edges, i.e., the attention that a token pays to other tokens. Note that each node may possibly have a different impact when voting. If the node itself is more important, the voting of this node is more important. This is shown in Algorithm 1. The transformation from initialization to convergence period is shown in Fig. 2(b).

# Algorithm 1 Graph-based Weighted Page Rank (WPR) algorithm

```
Require: N>0 is the number of nodes in the graph; A\in\mathbb{R}^{N\times N} is the adjacency matrix of this graph; s\in\mathbb{R}^N represents the graph signal Ensure: s\in\mathbb{R}^N represents the importance score of nodes in the graph s^0\leftarrow\frac{1}{N}\times e_N \Rightarrow Initialize the graph signal uniformly t\leftarrow0 \Rightarrow While (|s^t-s^{t-1}|>\epsilon) or (t=0) do \Rightarrow Continue iterating if not converged t\leftarrow t+1 s^t\leftarrow A^T\times s^{t-1} \Rightarrow Use the adjacency matrix as a graph shift operator end while s\leftarrow s^t
```

We obtain the expression for importance score of each node (i.e., token) in the l-th layer, h-th head as follows:

$$s^{(l)}(x_i) = \frac{1}{N_h} \frac{1}{N} \sum_{h=1}^{N_h} \sum_{j=1}^{N} \mathbf{A}^{(h,l)}(x_i, x_j) \cdot s^{(h,l)}(x_j)$$
 (1)

where  $s^{(l)}(x_i)$  is the importance score of node  $x_i$  in the l-th layer,  $N_h$  is the number of heads in the l-th layer, and N is the number of tokens in the l-th layer.  $s^{(h,l)}(x_j)$  is derived from the weighted sum of the received attention. Note that, after convergence, the vote, or attention, of the unimportant tokens is basically negligible. This is the advantage of the proposed WPR algorithm. It prevents the unimportant nodes from adding noise and affecting the final decision. We retain the top-k important tokens (k is a function of the retention rate of the pruning layer and the total number of tokens in the input sequence).

In the WPR algorithm, the importance scores of different heads are simply averaged. This is not necessarily the optimal choice. Different heads in an encoder layer usually pay attention to different parts of the input image (a visual example is given in Supplementery Material Section E.1). Thus, there are some tokens that are very important in one or two heads, but not in others. On the other hand, some tokens have low-to-medium importance in all heads. The former tokens are usually more informative than the latter tokens. However, if there are multiple heads and the importance score is directly averaged across all heads, the latter tokens may get the same or even higher score than the former tokens, leading to incorrect token ranking and pruning. In order to address this problem, we propose the Emphasizing Informative Pixels (EIP) technique. It replaces the original importance score  $s^{(l)}\left(x_i\right)$  with a root mean square of the importance scores of different heads. This can effectively distinguish informative pixels from non-informative ones. A concrete example that compares EIP with other methods (such as argmax and average) is given in Supplementary Material Section E.1.

Besides the issue mentioned above, sometimes the importance scores given by the WPR algorithm may converge to an undesired distribution in some heads: (1) tokens at the edge of the input image may get very high importance scores; (2) the importance score distribution may become nearly uniform. We provide visual examples of these cases in Supplementary Material Section E.2. Both of heads in these cases do not provide helpful information and are even misleading. To mitigate the negative impact of these heads, we introduce the Variance-based Head Filter (VHF). We compute the variance of the distribution in each head and set both a minimum and a maximum threshold for the variance. Heads with a distribution variance exceeding the maximum threshold or falling below the minimum threshold are excluded from the computation. Then the final importance score equation becomes:

$$s^{(l)}(x_i) = \frac{1}{N_h} \sqrt{\sum_{h=1}^{N_h} \left( \frac{1}{N} \sum_{j=1}^{N} \mathbf{A}^{(h,l)}(x_i, x_j) \cdot s^{(h,l)}(x_j) \right)^2 \cdot \eta \left( v_{\min} \le Var_h \le v_{\max} \right)}$$
 (2)

where  $\eta$  ( $v_{\min} \le Var_h \le v_{\max}$ ) equals 1 if  $v_{\min} \le Var_h \le v_{\max}$ , otherwise it equals 0;  $v_{\min}$  and  $v_{\max}$  represent the minimum and maximum threshold, respectively;  $Var_h$  is the importance score variance of tokens in the h-th head. Note that inference is not parallelizable if VHF is enabled.

## 3.3 S-stage: Similarity-based Pruning

Most previous token pruning methods solely rely on token importance to conduct pruning, disregarding the impact of similarity between tokens. However, a high importance score is not always indicative of a token's necessity. Fig. 3(a) shows a fish image, whose red-framed part is very important. If this part is masked, as shown in Fig. 3(b), we cannot identify what this image represents. This is also confirmed by the importance score distribution obtained by our graph-based WPR algorithm. However, if we mask the center of this fish, as shown in Fig. 3(c), it is still easy to identify this image as a fish, although the tokens in the center get high importance scores in our algorithm. This indicates that once some important tokens are selected, some other important tokens are no longer necessary.

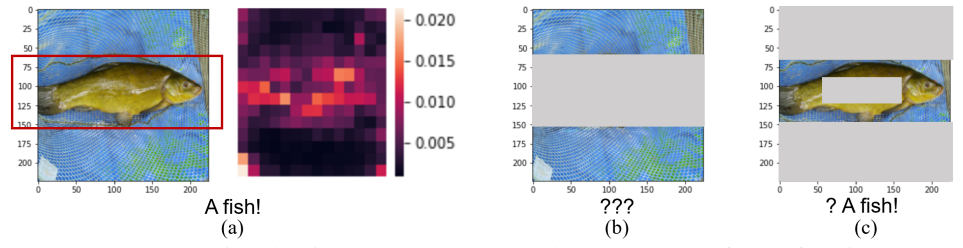


Figure 3: Example showing that important tokens may be unnecessary for performing a successful inference: (a) fish and its importance score distribution, (b) masked fish, and (c) partially masked fish. The above example illustrates that it is valuable to measure similarity between even important tokens and perform further pruning. ToMe [23] explores merging tokens according to the similarity between paired tokens, but the pattern of pairing and merging is solely based on the index of tokens, i.e., the location of corresponding patches in the input image. For different input images, the characteristics of paired tokens could be completely different, leading to unstable merging.

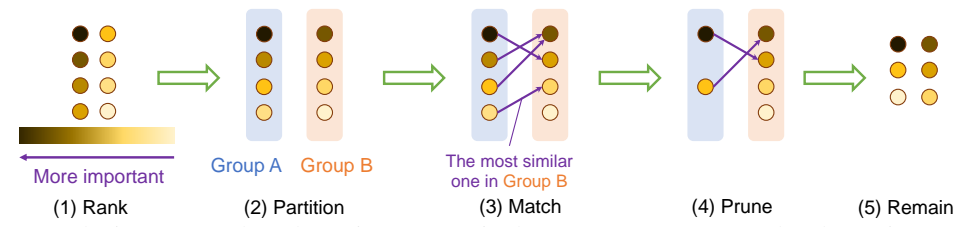


Figure 4: The importance-based pruning process in the S-stage. As an example, alternative partitioning is used in this figure.

To fix this issue, we propose an importance-guided partitioning, matching, and pruning process, as shown in Fig. 4. (1&2) Based on the importance score of tokens, we partition them into groups of roughly equal size, A and B. Multiple design choices are available here, including (i) partitioning alternatively, then the average token importance in two groups is nearly equal; (ii) partitioning sequentially, then tokens that are more important than average are in one group and other less important tokens are in another group; (iii) partitioning randomly. Ablation experiments indicate that partitioning sequentially and assigning less important tokens to group A is the best choice. We provide a quantitative comparison between them in Supplementary Material Section G.3. (3) We then identify the most similar token in Group B for each token in Group A and record the corresponding similarity of each pair. To accomplish this, each token is represented by a feature vector, which can be derived from several available choices, such as corresponding vectors in the Key, Query, or Value matrix. Our ablation experiments indicate that using vectors from the Key matrix is the optimal choice. Similarity is computed on these vectors using a designated metric, such as cosine similarity, Manhattan distance, or Euclidean distance. Following the results of our ablation experiments, we employ cosine similarity. We provide a detailed account of our ablation experiment outcomes in Supplmentary Material Section G.3. (4&5) In the next step, we select top-r similar pairs and prune corresponding tokens in Group A. We prune one token in each selected pair instead of merging them, due to the following reasons: (i) since tokens in the selected pairs are similar, pruning one of them results in only minimal information loss; (ii) merged tokens should have higher weights in the following computation [23], which makes it incompatible with certain backbones, such as Sparse Transformer [24]. Finally, remaining tokens are passed to the next stage.

The importance-guided partitioning in the **S-stage** facilitates stable control over the importance of the pruned tokens for different input images. By pruning similar tokens instead of merging them, our method maintains compatibility with certain specialized backbones [24] while incurring only minimal information loss.

# 4 Experimental Results

In this section, we present ablation experiments to validate our design choices and the effectiveness of our proposed methods. Then we compare Zero-TPrune with state-of-the-art token pruning methods.

**Experimental Setup:** To compare different pruning methods, we apply them to various vision Transformer backbones and evaluate the performance of pruned models on ImageNet [17]. Models are evaluated on 224px images unless otherwise noted. The inference GFLOPS of various pruned models are estimated on a single V100 GPU using the *fvcore* library provided by Meta<sup>1</sup>. Training (fine-tuning) after pruning is done on NVIDIA Tesla A100 40GB GPUs.

For ablation experiments, we implement Zero-TPrune on the DeiT-S model [16] with different configurations and design choices. For comparisons with state-of-the-art token pruning works, we divide them into two types: (1) methods that require fine-tuning of the pruned model, including DynamicViT [14] and A-ViT [15]; (2) fine-tuning-free methods, including ATS [21] and ToMe [23] (which is a token-merging instead of a token-pruning method, but is also fine-tuning-free). For the first type, we compare implementations on DeiT models. We use the official implementation of DynamicViT to reproduce its results and also generate some new ones for comparisons. For A-ViT, we directly use the results presented in that article. For the second type, we use the official open-source code of ATS and ToMe to implement them on various pre-trained Transformer backbones, including DeiT [16], LV-ViT [18], MAE [25], AugReg [26], and SWAG [27]. We compare off-the-shelf performance of Zero-TPrune with theirs. In addition, we compare the performance of pruned models on downstream tasks to check their transfer learning capability, following the selection of datasets in [28]. We provide details of the selected datasets in Supplementary Material Section F.

## 4.1 Ablation Experiments

We use ablation experiments to determine the optimal hyperparameters for Zero-TPrune. First, it is computationally expensive to check whether the WPR algorithm converges after each iteration. Thus, it would be desirable if we could determine the number of its iterations in advance. By checking the importance distributions after different numbers of iterations and computing the Kullback-Liebler (KL) divergence between them, we find 30-50, 5-10, and 1 iteration(s) are enough to ensure convergence in the first three layers, medium layers, and last three layers, respectively. Visual and quantitative comparisons are provided in Supplementary Material Section G.1. Second, we determine good enough minimum and maximum thresholds for VHF through random initialization and greedy search. We provide detailed search configurations and results in Supplementary Material Section G.2. The range found is [0.01,0.7], which is the default setting in our experiments unless otherwise noted. Third, we explore optimal design choices in the **S-stage** with ablation experiments presented in Supplementary Material Section G.3.

To illustrate the effectiveness of the different techniques employed in Zero-TPrune, we break down their contribution. We apply different combinations of techniques employed in Zero-TPrune to the DeiT-S model and evaluate the performance of the pruned models. Pruning layers are inserted after the [1,3,6,9,11]-th layer with a retention rate of [1,0.9,0.8,0.7,1] and #iterations of [30,5,5,1,1] in the **I-stage**, and 10 tokens are pruned in each **S-stage**. Before the **S-stage** is added, pruning layers are inserted after the [3,6,9,11]-th layer with a retention rate of [0.8,0.7,0.7,0.6] and #iterations of [5,5,1,1]. The results are shown in Table 1. We can see that the WPR algorithm improves the performance significantly. The EIP/VHF techniques and the **S-stage** improve the performance further.

Here, we employ Monto Carlo (MC) simulation to randomly explore the hyperparameter space, which includes the number and location of pruning layers, corresponding retention rates, number of iterations in each layer, and number of tokens to be pruned in each **S-stage**. After conducting thousands of trials, we select the optimal setting that exhibits the best performance achieved by Zero-TPrune while maintaining a fixed GFLOPS budget. To ensure a fair comparison, we do not use the MC simulation approach in Zero-TPrune in subsequent comparisons with state-of-the-art methods.

https://github.com/facebookresearch/fvcore

Table 1: Contribution breakdown of the different techniques employed in Zero-TPrune.

Acc@1	params	GFLOPS	Method
79.8% (base) 76.8% (-3.0%) 77.8% (+1.0%) 78.0% (+0.2%) 78.2% (+0.2%) 78.7% (+0.5%)	22M 22M 22M 22M 22M 22M 22M	4.55G 3.08G 3.08G 3.08G 3.08G 3.08G	Unpruned model random drop WPR WPR + EIP WPR + EIP + VHF (I-stage) I-stage + S-stage
78.9% (+0.2%)	22M	3.08G	I-stage + S-stage + MC Simulation

## 4.2 Comparison with State-of-the-Art Methods

In this section, the number and location of pruning layers are manually chosen with either constant or uniformly declining retention rates to match the given GFLOPS budget. The number of pruned tokens in each **S-stage** is kept constant. The number of iterations is fixed to 30, 5, and 1 for the first three layers, intermediate layers, and the last three layers, respectively.

**Comparison with Fine-Tuning-Required Methods:** To illustrate the advantages of Zero-TPrune, we compare its performance with that of DynamicViT and A-ViT with/without fine-tuning after pruning. Given the random initialization and the fact that pruning modules in DynamicViT and A-ViT need to be trained, the performance of DynamicViT and A-ViT without fine-tuning after pruning is based on randomly-pruned tokens.

Fig. 5 clearly demonstrates the advantages of Zero-TPrune over state-of-the-art fine-tuning-required Transformer pruning methods, i.e., DynamicViT and A-ViT. Without fine-tuning after pruning, Zero-TPrune outperforms DynamicViT and A-ViT (using random drop in this case) by around 1%. This means Zero-TPrune **reduces the accuracy drop by more than 60%**. The performance of Zero-TPrune without fine-tuning after pruning is comparable to that of DynamicViT and A-ViT with fine-tuning after pruning (e.g., 0.26% accuracy loss relative to the best, given a 3.5 GFLOPS budget on DeiT-S). With fine-tuning after pruning, Zero-TPrune outperforms both DynamicViT and A-ViT. Zero-TPrune can also be easily applied to larger models (e.g., given a 13.6 GFLOPS budget on DeiT-B) for higher accuracy. On the contrary, applying DynamicViT and A-ViT to large models is very computationally expensive due to their expensive fine-tuning (training) after pruning process.

Comparison with Fine-Tuning-Free Methods: ATS and ToMe provide an off-the-shelf option to prune Transformer models without the requirement of fine-tuning after pruning. We first apply them and Zero-TPrune to the DeiT-S model to compare off-the-shelf performance after pruning without fine-tuning. The results are shown in Fig. 6 and Table 2. As shown in Fig. 6, compared with state-of-the-art fine-tuning-free methods, Zero-TPrune reduces the accuracy loss by 31% on the DeiT-S model with a 3 GFLOPS budget. If we change the pruning configuration and give a higher budget (e.g., reduce GFLOPS by 20%), the accuracy loss introduced by Zero-TPrune is less than 0.4%. Zero-TPrune can reduce GFLOPS by 13% at nearly no cost. Note that these results are obtained without fine-tuning.

We further evaluate Zero-TPrune and baselines on various backbones with different sizes. The results are shown in Tables 3, 4, and 5. We find that when the original model is medium-sized, e.g., AugReg and LV-ViT-S, Zero-TPrune outperforms baseline methods by a large margin (it reduces accuracy loss by up to 45%). For large models, if the pruning is moderate (i.e., reduce GFLOPS by 20%), Zero-TPrune still outperforms baselines methods slightly. However, when large models are aggressively pruned (i.e., reduce GFLOPS by 50%), Zero-TPrune does not outperform baselines. Note that aggressively pruning large models is usually not a good idea. This point is indicated by the comparison between the optimal pruned LV-ViT-M model and the optimal pruned LV-ViT-S model. The latter requires only 60% of the GFLOPS at the cost of 0.1% accuracy loss. Compared with aggressively-pruned large models, scaling to a smaller model is often a better choice. We provide a detailed discussion of this fact in Supplementary Material Section H.

We also evaluated the performance of pruned models on downstream tasks to measure their transfer learning capability. Several small image datasets are selected. Zero-TPrune outperforms baselines on most datasets, indicating its strong transfer learning capability after pruning. We introduce selected datasets and present detailed experimental results in Supplementary Material Section F.

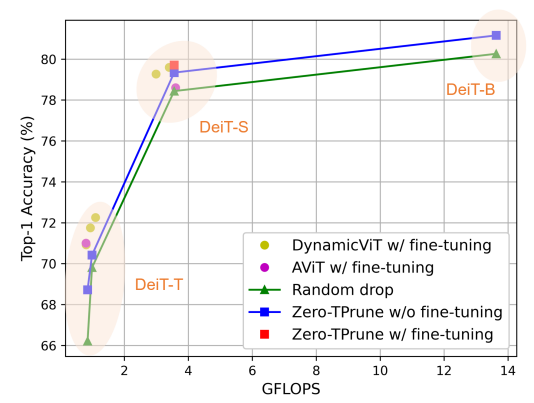


Figure 5: Performance comparison between Zero-TPrune and state-of-the-art fine-tuning-required methods.

Table 2: Performance of pruned DeiT-S models without fine-tuning.

Method	Acc@top1	GFLOPS
Unpruned	79.8%	4.55
ATS	78.2% (-1.6%)	3.03 (-33.4%)
ToMe	77.9% (-1.9%)	2.95 (-35.2%)
Zero-TP-a	<b>78.7% (-1.1%</b> )	3.08 (-32.5%)
Zero-TP-b	79.4% (-0.4%)	3.56 (-21.8%)
Zero-TP-c	79.7% (-0.1%)	3.97 (-12.7%)

Table 4: Performance of pruned LV-ViT models without fine-tuning.

Models	Acc@top1	GFLOPS
LV-ViT-S	83.3%	6.6
+ ATS	80.4%	3.5
+ ToMe	79.8%	3.6
+ Zero-TP	81.5%	3.5
LV-ViT-M	84.0%	12.7
+ ATS	80.9%	6.4
+ ToMe	81.6%	6.3
+ Zero-TP	81.4%	6.3

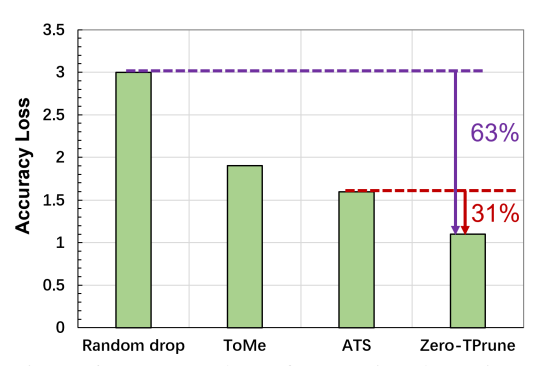


Figure 6: Accuracy loss after pruning the DeiT-S model with a 3 GFLOPS budget.

Table 3: Performance of pruned AugReg models without fine-tuning.

Acc@top1	GFLOPS
81.41%	4.55
79.21%	2.80
79.30%	2.78
80.22%	2.79
	81.41% 79.21% 79.30%

Table 5: Performance of pruned MAE and SWAG models without fine-tuning. SWAG models perform inference on 384x images.

Models	Acc@top1	GFLOPS
MAE	83.62%	55.4
+ATS-a	82.07%	42.3
+ToMe-a	82.69%	42.2
+Zero-TP-a	82.93%	42.3
+ATS-b	<b>79.21%</b>	29.1
+ToMe-b	78.95%	28.8
+Zero-TP-b	78.94%	28.6
SWAG	85.30%	55.6
+ATS	81.03%	27.8
+ToMe	84.59%	28.4
+Zero-TP	83.04%	28.3

## 5 Conclusion

In this article, we proposed Zero-TPrune, a zero-shot token pruning method that exploits both importance and similarity of tokens to eliminate the fine-tuning process after pruning. In the **I-stage**, it considers the attention matrix to be an adjacency matrix of an attention graph, which reduces noise from unimportant tokens. In the **S-stage**, it uses importance distribution to guide token matching and pruning, making them more stable and precise. Through the implementation of Zero-TPrune and baseline methods on various Transformer backbones and evaluation on ImageNet, we showed that it can eliminate the fine-tuning process after pruning with tiny accuracy reduction. Moreover, when compared to state-of-the-art off-the-shelf pruning methods, Zero-TPrune not only outperforms them by minimizing accuracy loss by up to 45%, but also enhances the transfer learning capability of pruned models. These findings emphasize the effectiveness of Zero-TPrune in balancing model compression and preservation of performance, making it a promising approach for efficient and accurate pruning of Transformer models. Future work can enhance the capabilities of Zero-TPrune further. One intriguing topic of study involves examining the applicability of Zero-TPrune to tasks such as image reconstruction, segmentation, and generation. Investigating the potential benefits and performance gains of employing Zero-TPrune in these domains holds promise for advancing the field.

# Acknowledgments and Disclosure of Funding

The work was supported by NSF under Grant No. CCF-2203399.

#### References

- [1] Szegedy, Christian, Wojciech Zaremba, Ilya Sutskever, Joan Bruna, Dumitru Erhan, Ian Goodfellow, and Rob Fergus. "Intriguing properties of neural networks." In 2nd International Conference on Learning Representations, 2014.
- [2] Devlin, Jacob, Ming-Wei Chang, Kenton Lee, and Kristina Toutanova. "BERT: Pre-training of deep bidirectional transformers for language understanding." *arXiv preprint arXiv:1810.04805*, 2018.
- [3] Schaal, Stefan, and Christopher G. Atkeson. "Learning control in robotics." *IEEE Robotics & Automation Magazine* 17, no. 2 (2010): 20-29.
- [4] Mnih, Volodymyr, Koray Kavukcuoglu, David Silver, Andrei A. Rusu, Joel Veness, Marc G. Bellemare, Alex Graves et al. "Human-level control through deep reinforcement learning." *Nature* 518, no. 7540 (2015): 529-533.
- [5] Vaswani, Ashish, Noam Shazeer, Niki Parmar, Jakob Uszkoreit, Llion Jones, Aidan N. Gomez, Łukasz Kaiser, and Illia Polosukhin. "Attention is all you need." Advances in Neural Information Processing Systems, 30 (2017).
- [6] Dosovitskiy, Alexey, Lucas Beyer, Alexander Kolesnikov, Dirk Weissenborn, Xiaohua Zhai, Thomas Unterthiner, Mostafa Dehghani, Matthias Minderer, Georg Heigold, Sylvain Gelly, Jakob Uszkoreit, Neil Houlsby. "An image is worth 16x16 words: Transformers for image recognition at scale." arXiv preprint arXiv:2010.11929, 2020.
- [7] Fedus, William, Barret Zoph, and Noam Shazeer. "Switch transformers: Scaling to trillion parameter models with simple and efficient sparsity." *Journal of Machine Learning Research*, 23 (2022) 1-39.
- [8] Michel, Paul, Omer Levy, and Graham Neubig. "Are sixteen heads really better than one?" *Advances in Neural Information Processing Systems*, 32 (2019).
- [9] Goyal, Saurabh, Anamitra Roy Choudhury, Saurabh Raje, Venkatesan Chakaravarthy, Yogish Sabharwal, and Ashish Verma. "PoWER-BERT: Accelerating BERT inference via progressive word-vector elimination." In *International Conference on Machine Learning*, pp. 3690-3699 (2020).
- [10] Kim, Gyuwan, and Kyunghyun Cho. "Length-adaptive transformer: Train once with length drop, use anytime with search." *arXiv preprint arXiv:2010.07003*, 2020.
- [11] Wang, Hanrui, Zhekai Zhang, and Song Han. "Spatten: Efficient sparse attention architecture with cascade token and head pruning." In *IEEE International Symposium on High-Performance Computer Architecture*, pp. 97-110, 2021.
- [12] Ye, Deming, Yankai Lin, Yufei Huang, and Maosong Sun. "TR-BERT: Dynamic token reduction for accelerating BERT inference." *arXiv preprint arXiv:2105.11618*, 2021.
- [13] Kim, Sehoon, Sheng Shen, David Thorsley, Amir Gholami, Woosuk Kwon, Joseph Hassoun, and Kurt Keutzer. "Learned token pruning for transformers." In *Proceedings of the 28th ACM SIGKDD Conference on Knowledge Discovery and Data Mining*, pp. 784-794, 2022.
- [14] Rao, Yongming, Wenliang Zhao, Benlin Liu, Jiwen Lu, Jie Zhou, and Cho-Jui Hsieh. "DynamicViT: Efficient vision transformers with dynamic token sparsification." Advances in Neural Information Processing Systems, 34 (2021): 13937-13949.
- [15] Yin, Hongxu, Arash Vahdat, Jose M. Alvarez, Arun Mallya, Jan Kautz, and Pavlo Molchanov. "A-ViT: Adaptive tokens for efficient vision transformer." In *Proceedings of the IEEE/CVF Conference on Computer Vision and Pattern Recognition*, pp. 10809-10818, 2022.
- [16] Touvron, Hugo, Matthieu Cord, Matthijs Douze, Francisco Massa, Alexandre Sablayrolles, and Hervé Jégou. "Training data-efficient image transformers & distillation through attention." In *International Conference on Machine Learning*, pp. 10347-10357, 2021.
- [17] Deng, Jia, Wei Dong, Richard Socher, Li-Jia Li, Kai Li, and Li Fei-Fei. "ImageNet: A large-scale hierarchical image database." In *IEEE Conference on Computer Vision and Pattern Recognition*, pp. 248-255, 2009.

- [18] Jiang, Zi-Hang, Qibin Hou, Li Yuan, Daquan Zhou, Yujun Shi, Xiaojie Jin, Anran Wang, and Jiashi Feng. "All tokens matter: Token labeling for training better vision transformers." Advances in Neural Information Processing Systems, 34 (2021): 18590-18602.
- [19] Bao, Hangbo, Li Dong, Songhao Piao, and Furu Wei. "BEiT: BERT pre-training of image transformers." In *International Conference on Learning Representations*, 2021.
- [20] Page, Lawrence, Sergey Brin, Rajeev Motwani, and Terry Winograd. "The PageRank citation ranking: Bringing order to the web." *Stanford InfoLab*, 1999.
- [21] Fayyaz, Mohsen, Soroush Abbasi Koohpayegani, Farnoush Rezaei Jafari, Sunando Sengupta, Hamid Reza Vaezi Joze, Eric Sommerlade, Hamed Pirsiavash, and Jürgen Gall. "Adaptive token sampling for efficient vision transformers." In 17th European Conference of Computer Vision, 2022.
- [22] Yuan, Li, Yunpeng Chen, Tao Wang, Weihao Yu, Yujun Shi, Zi-Hang Jiang, Francis E. H. Tay, Jiashi Feng, and Shuicheng Yan. "Tokens-to-token ViT: Training vision transformers from scratch on ImageNet." In Proceedings of the IEEE/CVF International Conference on Computer Vision, pp. 558-567, 2021.
- [23] Bolya, Daniel, Cheng-Yang Fu, Xiaoliang Dai, Peizhao Zhang, Christoph Feichtenhofer, and Judy Hoffman. "Token merging: Your ViT but faster." *arXiv preprint arXiv:2210.09461*, 2022.
- [24] Child, Rewon, Scott Gray, Alec Radford, and Ilya Sutskever. "Generating long sequences with sparse transformers." arXiv preprint arXiv:1904.10509, 2019.
- [25] He, Kaiming, Xinlei Chen, Saining Xie, Yanghao Li, Piotr Dollár, and Ross Girshick. "Masked autoencoders are scalable vision learners." In *Proceedings of the IEEE/CVF Conference on Computer Vision and Pattern Recognition*, pp. 16000-16009, 2022.
- [26] Steiner, Andreas, Alexander Kolesnikov, Xiaohua Zhai, Ross Wightman, Jakob Uszkoreit, and Lucas Beyer. "How to train your ViT?: Data, augmentation, and regularization in vision transformers." *arXiv* preprint arXiv:2106.10270, 2021.
- [27] Singh, Mannat, Laura Gustafson, Aaron Adcock, Vinicius de Freitas Reis, Bugra Gedik, Raj Prateek Kosaraju, Dhruv Mahajan, Ross Girshick, Piotr Dollár, and Laurens Van Der Maaten. "Revisiting weakly supervised pre-training of visual perception models." In *Proceedings of the IEEE/CVF Conference on Computer Vision and Pattern Recognition*, pp. 804-814, 2022.
- [28] Cao, Yun-Hao, Hao Yu, and Jianxin Wu. "Training vision transformers with only 2040 images." In 17th European Conference on Computer Vision, 2022.
- [29] Nilsback, M.-E., and Andrew Zisserman. "A visual vocabulary for flower classification." In IEEE Conference on Computer Vision and Pattern Recognition, vol. 2, pp. 1447-1454, 2006.
- [30] Parkhi, Omkar M., Andrea Vedaldi, Andrew Zisserman, and C. V. Jawahar. "Cats and dogs." In IEEE Conference on Computer Vision and Pattern Recognition, pp. 3498-3505, 2012.
- [31] Cimpoi, Mircea, Subhransu Maji, Iasonas Kokkinos, Sammy Mohamed, and Andrea Vedaldi. "Describing textures in the wild." In Proceedings of the IEEE Conference on Computer Vision and Pattern Recognition, pp. 3606-3613, 2014.
- [32] Quattoni, Ariadna, and Antonio Torralba. "Recognizing indoor scenes." In *IEEE Conference on Computer Vision and Pattern Recognition*, pp. 413-420, 2009.
- [33] Wah, Catherine, Steve Branson, Peter Welinder, Pietro Perona, and Serge Belongie. "The CalTech-UCSD Birds-200-2011 dataset." 2011.
- [34] Maji, Subhransu, Esa Rahtu, Juho Kannala, Matthew Blaschko, and Andrea Vedaldi. "Fine-grained visual classification of aircraft." *arXiv preprint arXiv:1306.5151*, 2013.
- [35] Krause, Jonathan, Michael Stark, Jia Deng, and Li Fei-Fei. "3D object representations for fine-grained categorization." In *Proceedings of the IEEE International Conference on Computer Vision Workshops*, pp. 554-561, 2013.
- [36] Cuturi, Marco, Olivier Teboul, and Jean-Philippe Vert. "Differentiable ranking and sorting using optimal transport." In *Advances in Neural Information Processing Systems* 32, 2019.

# **Supplementary Material**

## A The I-S Pattern and the I'-S-I Pattern

In this section, we first demonstrate the *overwhelming of the major group* issue caused by the I-S pattern and then compare it with the I'-S-I pattern visually.

## A.1 Overwhelming of the Major Group with the I-S Pattern

Sometimes, unimportant parts of an image may be identified as important and important parts as unimportant by our graph-based WPR algorithm. An example is shown in Fig. 7. It shows that the background of the image is considered important in the Transformer heads. The fish itself, surprisingly, is considered unimportant.

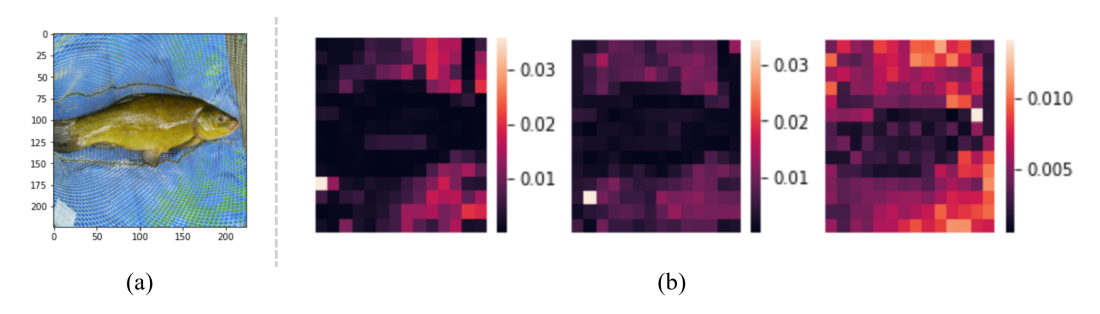


Figure 7: An example illustrating that a large unimportant group may overwhelm a small important group: (a) input image and (b) three examples showing that unimportant background tokens overwhelm the important fish tokens.

In this image, the *background* and *fish* tokens form two sets: A and B. In the beginning, because tokens in *set* B are more important than those in *set* A, they have relatively high importance scores. However, both tokens in *set* A and *set* B mainly intend to vote for tokens in their own set. Thus, it is easier for *set* A to form tokens with high importance scores because *set* A includes more tokens. These "highly important" tokens have larger voting weights in the next iteration. This makes it even easier for other tokens in *set* A to get "high importance." This is a positive feedback loop, with the result that the most "important" tokens end up in *set* A.

#### A.2 Comparison

As shown in Fig. 8, by pruning similar background tokens in advance, the *overwhelming of the major group* problem is alleviated significantly.

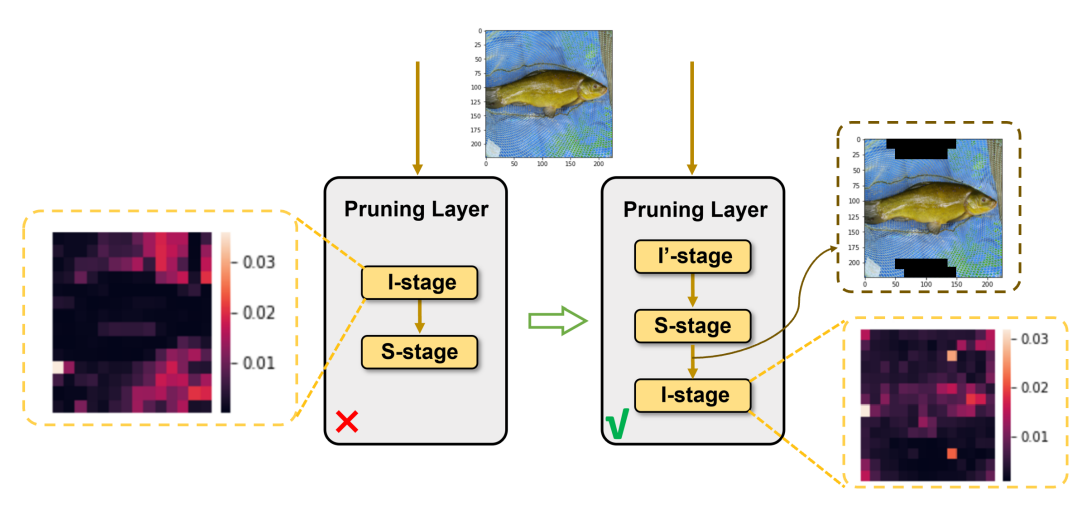


Figure 8: Visual comparison between the I-S pattern and the I'-S-I pattern.

# **B** Attention Probability Matrix

ViT [6] and its variants contain multiple Transformer encoder layers that are stacked up together. The basic Transformer encoder layer includes a multi-head attention (MHA) block followed by a feed-forward network (FFN) block, with residual connections and layer normalization around each. We make the assumption that an MHA block consists of H independently parameterized heads. An attention head h in layer l can be parameterized by the Key, Query, and Value weight matrices:  $\mathbf{W}_k^{(h,l)}, \mathbf{W}_q^{(h,l)}, \mathbf{W}_v^{(h,l)} \in \mathbb{R}^{d_h \times d}$ , and the output weight matrix  $\mathbf{W}_o^{(h,l)} \in \mathbb{R}^{d \times d_h}$ , where  $d_h$  is typically set to d/H and d is the embedded feature dimension. Suppose  $x \in \mathbb{R}^{d \times n}$  is the input sequence and n is the input sequence length. For each head, the *attention probability* between token  $x_i$  and  $x_j$  is given as an element of matrix  $\mathbf{A}^{(h,l)}$ :

$$\mathbf{A}^{(h,l)}(x_i, x_j) = \operatorname{softmax}\left(\frac{x^T \mathbf{W}_q^T \mathbf{W}_k x}{\sqrt{d}}\right)_{(i,j)} \in \mathbb{R}$$
(3)

An example  $A^{(h,l)}$  is shown in Fig. 9. It is for an encoder layer in BERT [2] for the sentence "This is the best restaurant, and I will be returning for another meal." We can see that words "best," "restaurant," "returning," "another" are considered more important than the other words. When tokens are pruned, this matrix becomes smaller.

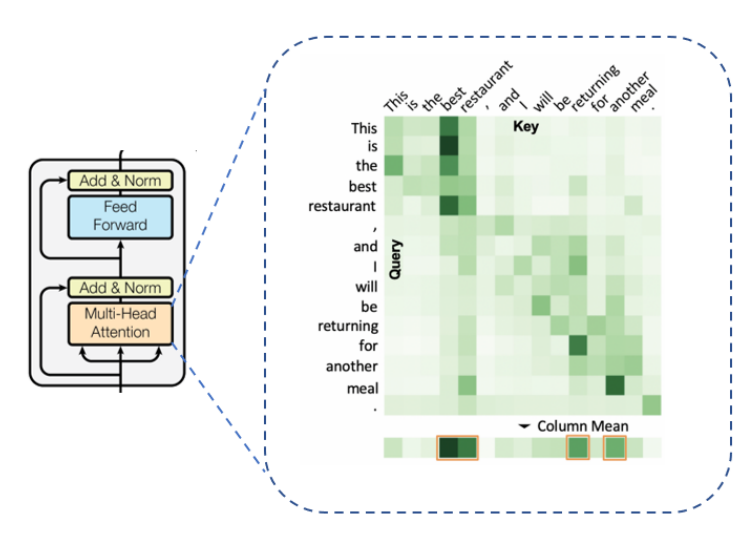


Figure 9: An example attention probability matrix [13].

This matrix measures how much token  $x_j$  attends to token  $x_i$ . The output of an MHA block can be formulated as follows:

$$x_{\text{MHA}} = \text{LN}\left(\mathbf{W}_o \sum_{i=1}^{n} \mathbf{W}_v x_i \mathbf{A}^{(h,l)} \left(x_i, x_j\right) + x\right)$$
(4)

The output of a Transformer encoder layer can be formulated as follows:

$$x_{\text{out}} = \text{LN}\left(\sigma\left(\mathbf{W}_{2}\left(\mathbf{W}_{1}x_{\text{MHA}} + b_{1}\right)\right) + b_{2} + x_{\text{MHA}}\right) \tag{5}$$

where  $\mathbf{W}_1$ ,  $\mathbf{W}_2$ ,  $b_1$ , and  $b_2$  are FFN parameters, and  $\sigma$  and LN denote the activation function and layer normalization, respectively. We can see that the computation overhead of a Transformer encoder layer undergoes a quadratic reduction when tokens are pruned.

# C Optional Training Paradigm after Pruning

Zero-TPrune can eliminate the fine-tuning process after pruning with tiny accuracy reduction. However, in some scenarios, we may have adequate samples and computational resources. In such cases, the performance of Zero-TPrune can be improved further by training (fine-tuning) after pruning. In this section, we introduce techniques used to accomplish this.

Given that it is very expensive to make importance-based ranking differentiable [36], we eliminate the **S-stage** and retain only the **I-stage** when we aim to further train (fine-tune) the pruned model. Besides this, to make Zero-TPrune differentiable, it is necessary to replace normal token pruning with "soft token pruning." Instead of completely discarding pruned tokens, soft token pruning assigns them small weights to reduce their effect on later computation and preserves compatibility with back-propagation during training. In this way, the non-differentiable token mask M is replaced with a differentiable soft mask  $\tilde{M}$  using the sigmoid operation:

$$\tilde{M}^{(l)}(x_i) = \sigma\left(\frac{s^{(l)}(x_i) - \theta^{(l)}}{T}\right) \tag{6}$$

where  $s^{(l)}(x_i)$  is the importance score of token  $x_i$  and  $\theta^{(l)}$  is the importance threshold for the l-th layer.  $\theta^{(l)}$  is determined based on the chosen pruning rate and GFLOPS budget. Details of soft token pruning can be found in [13].

For simplicity, we use a similar loss function to DynamicViT [14], which includes three terms:

$$\mathcal{L} = \mathcal{L}_{\text{cls}} + \lambda_{\text{distill}} \mathcal{L}_{\text{distill}} + \lambda_{\text{KL}} \mathcal{L}_{\text{KL}}$$
 (7)

The first term is the standard classification cross-entropy loss:

$$\mathcal{L}_{\text{cls}} = \text{CrossEntropy}(\mathbf{y}, \overline{\mathbf{y}})$$
 (8)

During fine-tuning, we use the original backbone network as the teacher model and push the behavior of the Zero-TPrune model to be as close to the teacher model as possible. First, we push the finally retained tokens of Zero-TPrune close to the ones of the teacher model. This contributes to the second distillation term above. We also minimize the difference in predictions between Zero-TPrune and its teacher via Kullback-Liebler (KL) divergence. This contributes to the third term. Details of the loss function can be found in [14].

## **D** Visualization

In this section, we use some visualization examples to provide high-level insights.

# D.1 An Input Image Example

Fig. 10 shows a simple test sample of a *fish* from the ImageNet dataset and the corresponding importance score distributions in different layers and heads. We can see that most heads can successfully capture the important part of this image with the help of the graph-based WPR algorithm.

## D.2 Averaged Importance Distribution over Thousands of Images

Another interesting visualization example is related to the general functionality of different layers in the Transformers. Fig. 11 shows the importance score distributions averaged over thousands of images. It indicates that different layers of the Transformer behave differently. Shallow layers focus more on the edge of input images and deep layers focus more on the center.

# **E** Combining Results of Different Heads

In this section, we introduce the techniques we propose to nontrivially combine the importance score distribution of different heads from the WPR algorithm.

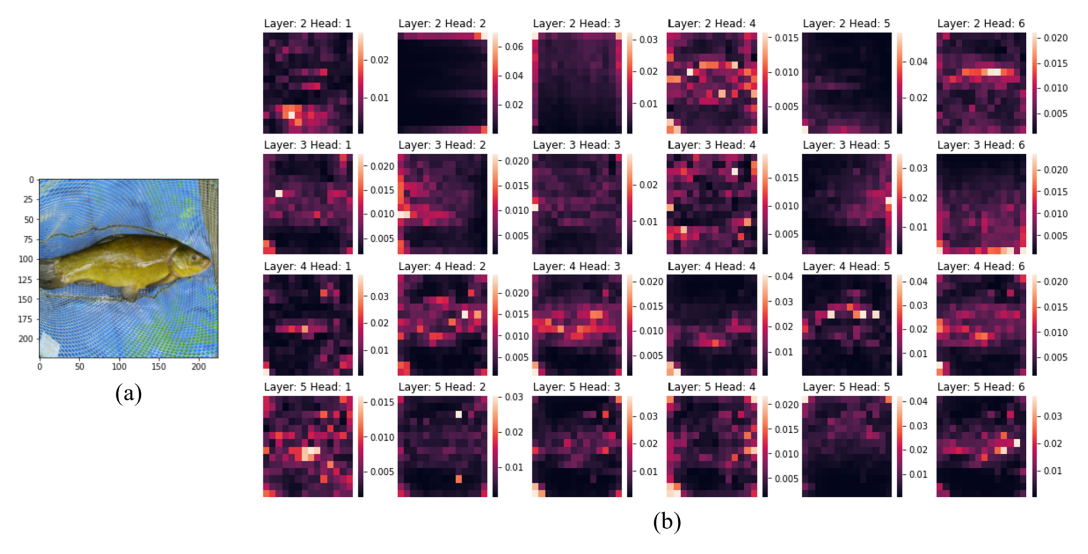


Figure 10: The important part of input images can be successfully captured by the graph-based WPR algorithm: (a) a test sample of *fish* in the ImageNet dataset and (b) the corresponding importance score distributions given by the WPR algorithm in different layers. The used backbone is DeiT-S.

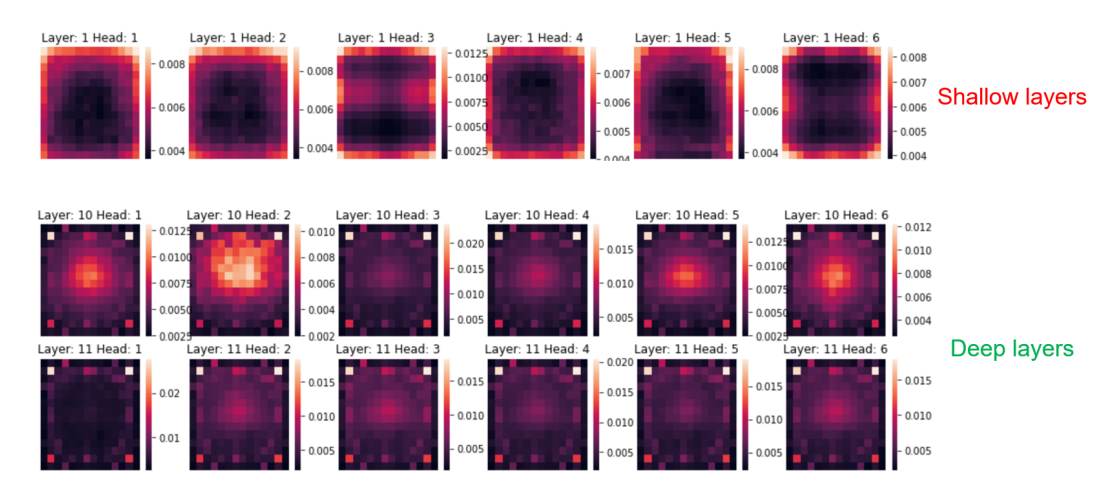


Figure 11: Importance score distributions averaged over thousands of images. The first row is derived from the first layer and the second (third) row from the 10th (11th) layer of the DeiT-S model.

## **E.1** Emphasizing Informative Pixels

Different heads in an encoder layer usually pay attention to different parts of the input image, as shown in Fig. 12. For the input image of a boy holding a fish, some heads pay more attention to the body of this boy, some to the head of this boy, and some to the fish in hand.

We propose EIP to address this issue. Suppose there are three heads in all and the importance scores of tokens A, B, and C are [9,9,9], [9,0,0], [3,3,3], respectively. The ideal importance order is A>B>C. Table 6 shows the outcome of application of different importance score calculation methods. The traditional averaging method assigns the same importance to tokens A and B. If we only select the highest score across all heads, tokens A and B will be assigned the same importance, which is also not desired. The proposed EIP technique balances the two situations and results in the ideal importance order.

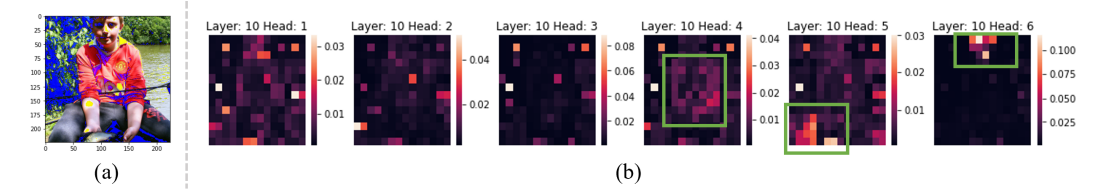


Figure 12: The distribution of importance score from different heads for an input image: (a) an image of a boy holding a fish and (b) importance score distributions. The results are obtained by the WPR algorithm with 30 iterations in the tenth layer of the DeiT-S model.

Table 6: Application of different importance score calculation methods to the example.

Importance Score	Average $\{S_i\}$	$max\{S_i\}$	EIP
Token A	9	9	5.2
Token B	3	9	3
Token C	3	3	1.7
Rank	A > B = C	A = B > C	A > B > C

#### E.2 Variance-based Head Filter

The importance scores given by the WPR algorithm may converge to an undesired distribution. Two typical examples are shown in Fig. 13. Tokens at the edge of the input image get very high importance scores in Fig. 13(b) and the importance score distribution in Fig. 13(c) is nearly uniform. We introduce VHF to mitigate the negative impact of these heads.

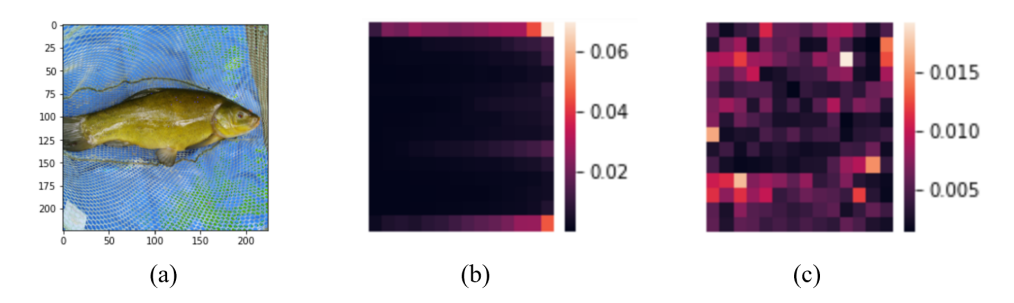


Figure 13: Examples of undesired importance score distributions in certain heads obtained by the WPR algorithm: (a) input image, (b) second head in the second layer of the DeiT-S model, and (c) fourth head in the third layer of the DeiT-S model.

## F Downstream Tasks

Table 7 shows the number of categories and test instances in the selected datasets. DTD is a describable textures dataset; Indoor67 is an indoor scene recognition dataset; CUB200 is a challenging dataset of 200 bird species. The other datasets have self-explanatory names.

The experimental results are shown in Table 8. Zero-TPrune outperforms baselines on most datasets, indicating its strong transfer learning capability after pruning. ToMe has worse performance on small-sized models due to a lack of enough layers to merge tokens gradually.

## **G** Ablation Experiments

In this section, we show results for further ablation experiments we performed.

Table 7: Datasets for downstream image classification.

Datasets	#Categories	#Test Instances
Flowers [29]	102	6149
Pets [30]	37	3669
DTD [31]	47	1880
Indoor67 [32]	67	1340
CUB200 [33]	200	5794
Aircrafts [34]	100	3333
Cars [35]	196	8041

Table 8: Performance of pruned models on downstream tasks.

Model	GFLOPS	Flowers	Pets	DTD	Indoor67	CUB200	Aircrafts	Cars
Deit-T	1.26	97.3	88.6	73.2	75.6	76.8	78.7	90.3
+ ATS	0.90	94.6	86.1	71.0	72.9	73.8	76.0	88.4
+ ToMe	0.90	93.2	84.7	69.9	71.6	72.9	75.2	87.1
+ Zero-TP	0.91	95.1	86.9	70.9	73.7	74.4	<b>76.7</b>	88.2

# G.1 Convergence Speed of the WPR Algorithm

It is computationally expensive to check whether the WPR algorithm converges after each iteration. Thus, it would be desirable if we could determine the number of its iterations in advance. In order to do so, we need to derive the general convergence behavior of the WPR algorithm. Fig. 14 shows the importance score distributions of tokens in 2,560 images. In the shallow layers, such as the first layer, the distributions corresponding to 30 iterations and five iterations are obviously different. This indicates that five iterations are not enough to make the WPR algorithm converge in the shallow layers. On the other hand, in the deep layers, such as the 12th layer, the distribution corresponding to 30 iterations is quite similar to the distribution corresponding to just one iteration. This means that one iteration is enough to make the WPR algorithm converge in the deep layers. In addition, in the fifth layer, five iterations are enough to make it converge.

To quantitatively verify the assertions we made above, we calculate the KL divergence between the importance distribution given by 30, 5, 1 iteration(s) and that given by 50 iterations in different layers. The results are shown in Fig. 15. Thus, to ensure convergence, we set the number of iterations to 30-50, 5-10, and 1 in the first three layers, medium layers, and last three layers, respectively. Another interesting thing to note is that the Transformer model and the WPR algorithm assign low-importance scores to most tokens in the deep layers.

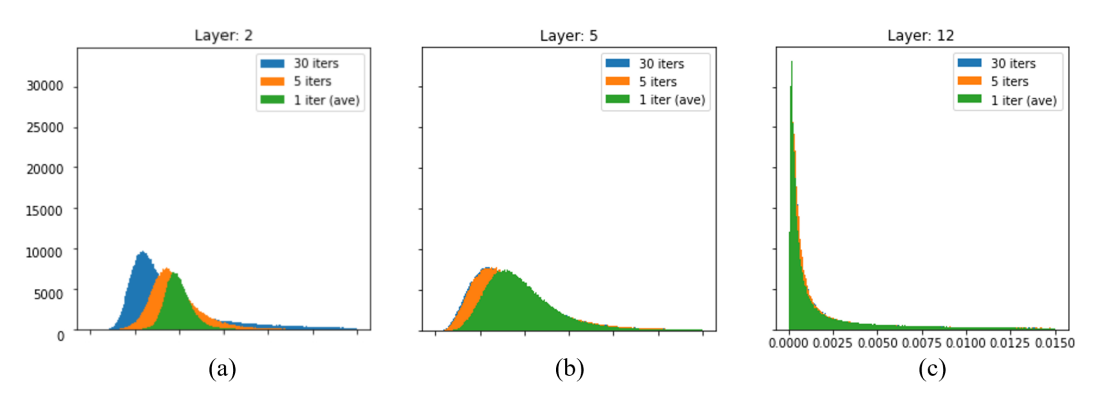


Figure 14: The importance score distributions of tokens in 2,560 images. The distribution changes with both the number of iterations and layer location: (a) layer 2, (b) layer 5, and (c) layer 12 in DeiT-S.

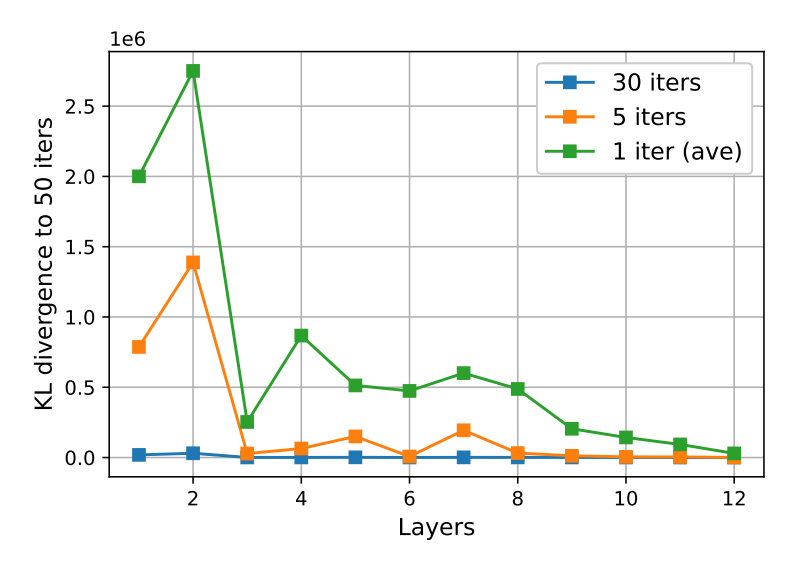


Figure 15: The KL divergence between the importance score distribution given by different numbers of iterations and that given by 50 iterations in different layers. The used backbone is DeiT-S.

## **G.2** Variance Thresholds for VHF

To exclude the noise from heads that converge to undesired importance score distributions (as shown in Fig. 13), we propose VHF and set minimum and maximum thresholds for the variance of head distributions. We perform an ablation experiment to determine the optimal variance range. The pruning configuration is shown in Table 9. We then use random initialization and beam search (k=2) to find a good enough variance range setting. The results are shown in Fig. 16, which points to the range [0.01,0.7].

Table 9: Pruning configuration used to search for optimal variance thresholds.

Pruning Layers	0	2	4	6	8	10
Retention Rates	0.9	0.9	0.85	0.8	0.7	0.65
# Iterations	50	50	5	5	1	1

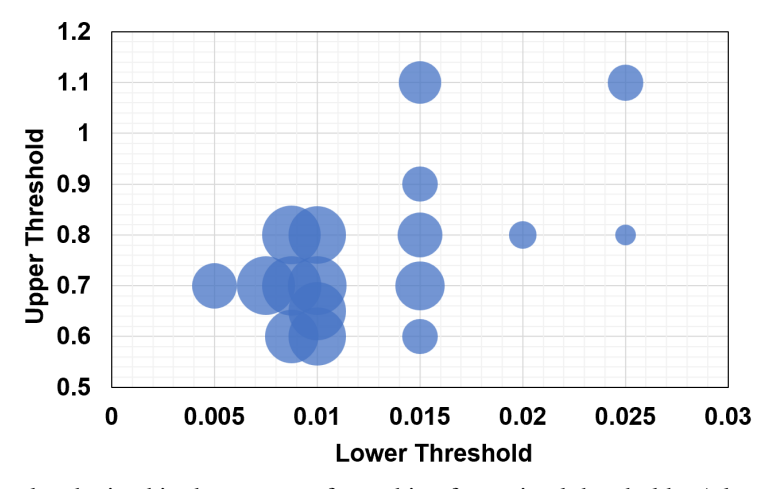


Figure 16: Results obtained in the process of searching for optimal thresholds. A larger blue bubble represents higher accuracy with that setting.

#### **G.3** Optimal Design Choices in the S-stage

As discussed in Section 3.3, the design space of the **S-stage** is composed of three dimensions: (1) source of feature vectors, (2) partitioning method, and (3) similarity metric. We find that the optimal choice is (1) key matrix, (2) sequential (prune unimportant part), and (3) cosine similarity, respectively. This is the default setting in the following experiments unless otherwise noted. For the results in this section, pruning layers are inserted after the [1,3,6,9,11]-th layer with a retention rate of [1,0.9,0.8,0.7,1] and #iterations of [30,5,5,1,1] in the **I-stage**, and 10 tokens are pruned in each **S-stage**.

**Feature vectors:** As shown in Fig. 17, feature vectors that represent tokens can be the corresponding vectors in the Key matrix, Query matrix, Value matrix, intermediate embedding vectors in the  $X_{pre}$  matrix, or output embedding vectors in the X matrix. We maintain the other settings and change the feature vectors used. The performance of pruned models is shown in Table 10. It indicates that the Key matrix is the optimal source of feature vectors.

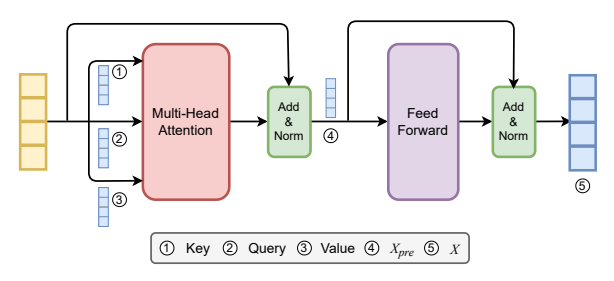


Figure 17: Potential feature vectors that can be used to represent tokens.

Table 10: Ablation experiment results for the source of **feature vectors**.

Feature	Acc@top1	GFLOPS
$egin{array}{c} { m X}_{pre} \ { m X} \end{array}$	78.318%	3.08
X	78.384%	3.08
K	<b>78.696</b> %	3.08
Q	78.378%	3.08
V	78.314%	3.08

**Partitioning method:** After ranking tokens according to their importance, we choose from the following options: (i) alternatively assign them to Group A and B, (ii) assign the less important half of tokens to Group A and the other half to Group B, which means we sequentially partition tokens and prune the unimportant part, (iii) assign the more important half of tokens to Group A and the other half to Group B, (iv) randomly assign them to Group A or B, and (v) assign all tokens to both groups without partitioning. To evaluate the effectiveness of these options, we conducted experiments while keeping all other settings at default values. The results are shown in Table 11, where Sequential-U represents choice (ii) and Sequential-I represents choice (iii). It clearly indicates that Sequential-U is preferable to all the other partitioning methods.

Similarity metric: We experimented with several metrics for measuring the similarity between two vectors, including cosine similarity, dot product, and Minkowski distance with different p values. When using Minkowski distance to measure similarity between vectors, we negated the distance to account for the fact that a longer distance indicates a lower similarity. The results of these experiments, shown in Table 12, indicate that cosine similarity is the best choice.

Table 11: Ablation experiment results for choosing the **partitioning method**.

Method	Acc@top1	GFLOPS
Random	78.462%	3.08
Alternate	78.494%	3.08
Sequential-U	<b>78.696</b> %	3.08
Sequential-I	78.298%	3.08
No partition	77.746%	3.08

Table 12: Ablation experiment results for choosing the **similarity metric**.

Similarity	Acc@top1	GFLOPS
dot product	78.310%	3.08
cosine	<b>78.696</b> %	3.08
Manhattan $(p=1)$	78.330%	3.07
Euclidean $(p=2)$	78.342%	3.07
Minkowski $(p=3)$	78.460%	3.07
Minkowski $(p=4)$	78.502%	3.07
Minkowski ( $p = 5$ )	78.414%	3.07
Minkowski ( $p = \infty$ )	78.358%	3.07

# H Comparison between Scaling and Pruning

Zero-TPrune cannot outperform baseline methods when a relatively high pruning rate (e.g., reduce GFLOPS by 50%) is applied to large models (e.g., DeiT-L). However, in this case, scaling to a smaller model is often a better choice. ToMe outperforms Zero-TPrune when large models are aggressively pruned. Thus, we use the results from ToMe to illustrate this point.

In Fig. 18, ToMe is applied to different ViT backbones with different configurations. Different points on the same curve represent different configurations applied to the same backbone. The first point from the left on each curve represents the unpruned model. Aggressively pruning a model implies switching from the first point from the left on a given curve to the last point on this curve, which increases throughput but suffers from lower accuracy. Switching from the first point from the left on a given curve to the first point on another curve directly scales the size of the model without pruning. As shown in Fig. 18, for large models (ViT-L and ViT-B), aggressively pruning them underperforms scaling them in terms of both accuracy and throughput. On the contrary, for the ViT-S model, although scaling outperforms aggressive pruning in terms of throughput, it achieves lower accuracy than aggressive pruning.

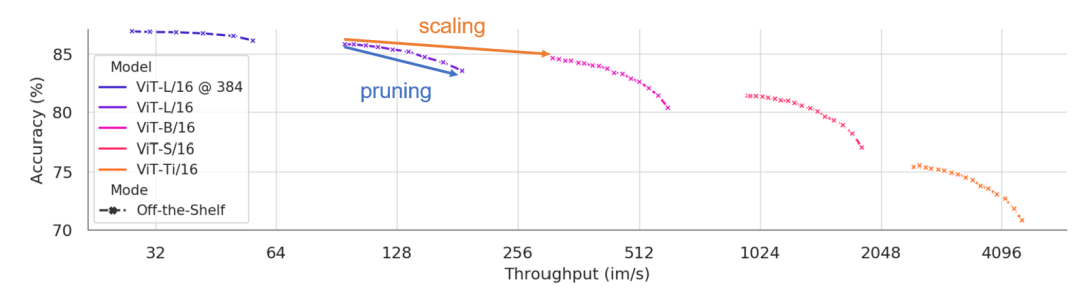


Figure 18: The off-the-shelf performance of ViT models under ToMe [23].